Int J Fract (2007) 143:355–367
DOI 10.1007/s10704-007-9068-3

ORIGINAL PAPER

A practical stress analysis for predicting fatigue limit of metal with axisymmetric complex surface

Tatsujiro Miyazaki · Yuuta Aono · Hiroshi Noguchi

Received: 16 July 2005 / Accepted: 14 March 2007 / Published online: 1 June 2007

Abstract In order to predict the fatigue limit of a specimen with an axisymmetric complex surface, a practical method to estimate a stress concentration factor (SCF) of its surface was proposed. The roughness is coarse-grained by removing high frequency components and approximated with a parallel row of a local notch and innumerable average notches. Then, the notches are each approximated with the elliptical holes in the infinite plate, and the SCF is calculated approximately by superposing the elastic solutions of the holes. Moreover, FEM analyses were carried out on the various notch models which consist of the local notch and innumerable average notches to examine the application limit of the present method. Then, the validity of the application limit was examined by using the real roughness and the infinite parallel row of the various notches, and it was shown that the present method was available for the real roughness.

Keywords Fatigue · Notch · Stress concentration · Body force method · Finite element method · Surface roughness · Fatigue limit

T. Miyazaki (✉)
University of the Ryukyus, Nishihara, Nakagami-gun, Okinawa 903-0213, Japan

Y. Aono · H. Noguchi
Kyushu University, 744 Motooka, Nishi-ku, Fukuoka 819-0395, Japan

1 Introduction

When there are several concavities and convexities in a surface, they interfere with each other and complex stress concentrations are formed there. If the same notches are arranged linearly and periodically in the surface, the stress concentration of the surface decreases depending on the interval between the notches. The phenomenon is called "Entlastung effect" (Neuber 1958) and some researchers have studied it (Neuber 1958; Hirano 1950; Nishihara and Fujii 1951; Isibasi 1954). However, the stress concentration of the complex surface without a reappearance and periodicity has not been clarified yet.

Murakami et al. approximated a periodic surface roughness with an infinite parallel row of small cracks and proposed the method for predicting the fatigue limit of a metal with such a surface by $\sqrt{\text{area}}$ parameter model, where area is a projected area of three dimensional crack to a plane perpendicular to a loading axis (Murakami et al. 1996; Murakami et al. 1997; Murakami 2002). And then, they carried out several fatigue tests on specimens with the various periodic surface roughnesses and examined the validity of the method by the experimental results. Also, the authors proposed the method to determine the stress concentration factor (SCF) of a complex surface profile with a sufficiently long periodicity by the extended Hirono's conformal mapping function (Hirano 1950; Aono and Noguchi 2004). Moreover, the authors proposed the method to

predict the fatigue limit reliability by approximating the complex profile with a unit crack or notch and examined the validity of the method by comparing the predicted results with experimental results of the specimens with the various complex two dimensional surfaces (Aono and Noguchi 2004). However, because the real surface roughness has three dimensional shape and does not have the periodicity and reappearance, the method which can be applied to the general surface with three dimensional shape is required.

In this study, for a prediction of a fatigue limit, an approximate method to calculate a SCF of two dimensional complex surface roughness is proposed. Concretely, it is supposed that the strength of a rough specimen obeys the weakest link model (Weibull 1951). Then, three concavities which may become the fatigue fracture origin are chosen from the mechanical profile (Aono and Noguchi 2004). One of them is assumed as the local notch, all of the concavities except for the local notch are assumed as infinite parallel row of the average notches. And the complex mechanical profile is approximated with the parallel row of the local notch and innumerable average notches. Three SCFs and fatigue limits are each calculated in turn independently. Finally, the minimum value of the predicted fatigue limits is adopted as the fatigue limit. Aono and Noguchi have reported that the complex roughness profile can be replaced with the unit notch or crack model and its fatigue limit can be predicted if the SCF and ρ are calculated appropriately. In this study, because the ρ is obtained easily, the method for calculating the SCF is discussed mainly. Moreover, the validity of the present method and its application limit are examined by a finite element simulation.

2 Fatigue limit of notched specimen of a metal

In general, when fatigue tests are carried out on notched specimens with constant notch depth t and various root radii ρ, a typical relation between fatigue limits and ρ is shown in Fig. 1 (Isibasi 1954). The ρ_0 in Fig. 1 is a limit notch root radius whether or not a nonpropagating macrocrack exists along the notch root at the fatigue limit. It is a material constant called "branch point" (Isibasi 1954; Nisitani 1983).

When $\rho > \rho_0$, the limit stress for the non-propagating microcrack, σ_{w1}, appears as the fatigue limit (Isibasi 1954; Nisitani 1972). The Linear Notch

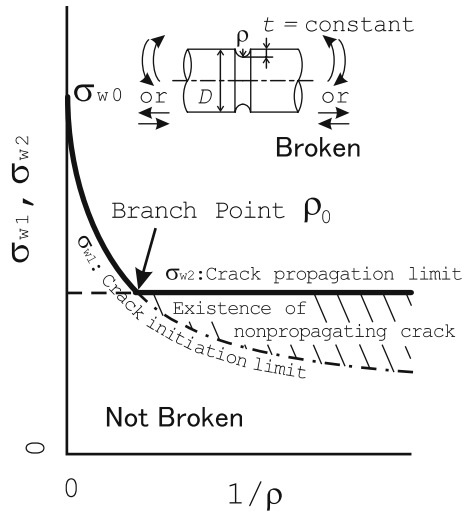

Fig. 1 Schematic illustration of a relation between fatigue limit and notch root radius

Mechanics is effective to predict the σ_{w1} (Nisitani 1972). Because the stress field near the notch root has a unique form which is governed by the SCF K_t and ρ, the σ_{w1} is predicted by the following equation (Miyazaki et al. 2004).

$$\sigma_{w1} = \frac{\sigma_{w0}}{K_t}\sqrt{1+\frac{230}{H_V^{1.46}\rho}} \tag{1}$$

$$\sigma_{w0} = 1.6\,H_V \tag{2}$$

(σ_{w0}, σ_{w1} : MPa , H_V : kgf/mm^2 , ρ : mm)

Here, H_V is a micro Vickers hardness, σ_{w0} is the fatigue limit of the plain specimen (Isibasi 1954; Murakami 2002).

On the other hand, when $\rho \le \rho_0$, the limit stress for the non-propagating macrocrack, σ_{w2}, appears as the fatigue limit. Shown in Fig. 1, the σ_{w2} is independent of ρ. Because the fatigue limit of the notched specimen with $\rho \le \rho_0$ is obtained from that of a cracked specimen whose crack depth is equal to t, the Linear Fracture Mechanics is effective to predict the σ_{w2}. Especially, when the notch depth is shallow enough, the σ_{w2} is predicted by the following equation (Murakami 2002).

$$\sigma_{w2} = \frac{1.43\,(H_V+120)}{\sqrt{\text{area}}^{1/6}} \tag{3}$$

(σ_{w2} : MPa , H_V : kgf/mm^2 , $\sqrt{\text{area}}$: μm)

Here, the relation between $\sqrt{\text{area}}$ and t is approximately expressed with the following equation (Murakami 2002).

$$\sqrt{\text{area}} = \sqrt{10}\, t \tag{4}$$

From Fig. 1, the fatigue limit of the notched specimen, σ_w, is predicted by the following equation.

$$\sigma_w = \max(\sigma_{w1}, \sigma_{w2}) \tag{5}$$

3 Coarse-graining of roughness and transformation from roughness to a notch and a crack

3.1 Coarse-graining of roughness

It is well known that a defect has a size effect on the fatigue limit (Murakami 2002). When the lower limit of the size is denoted with $\sqrt{\text{area}_c}$, it is obtained by solving $\sigma_{w2} = \sigma_{w0}$ on $\sqrt{\text{area}}$ as follows.

$$\sqrt{\text{area}_c} = \left\{ \frac{1.43\,(H_V + 120)}{1.6 H_V} \right\}^6 \tag{6}$$

When the crack is assumed to be two dimensional, its crack depth c_{IE} is approximately given by the following equation (Murakami 2002).

$$c_{IE} = \frac{\sqrt{\text{area}_c}}{\sqrt{10}} \tag{7}$$

Generally, the roughness profile can be expressed by the superposition of several profiles with various frequencies and spectra. Because the crack whose depth is smaller than c_{IE} has no effect on the fatigue limit, the roughness profile can be coarse-grained, keeping the same mechanical condition by removing the profiles whose amplitudes are smaller than c_{IE} (Aono and Noguchi 2004). Concretely, the high frequency profiles are removed from the roughness profile so as to meet the following equation.

$$|R(x) - W(x)| < c_{IE} \tag{8}$$

Here, $W(x)$ is a mechanical profile, $R(x)$ is a roughness profile. The coarse-grained surface roughness is called the mechanical profile (Aono and Noguchi 2004).

3.2 Transformation roughness to a notch and a crack

Figure 2 shows a schematic illustration of a transformation from the mechanical profile to a unit notch and crack model (Aono and Noguchi 2004). When $\rho > \rho_0$, the non-propagating microcrack limit σ_{w1} becomes the fatigue limit. Because the non-propagating behavior of the microcrack is governed by the stress field near the notch root, the mechanical profile is approximated with the unit notch model which has the stress field equal to that of the profile. The stress field near the notch root is determined by the K_t and ρ approximately. As shown in Fig. 2, the equivalent notch depth t_{eq} is introduced and determined so as to meet $K_{tA} = K_{tB}$ with the ρ constant, where K_{tA} and K_{tB} are the SCFs of the mechanical profile and the unit notch model, respectively. By using the t_{eq}, the mechanical profile can be expressed with the unit notch model keeping the mechanical condition.

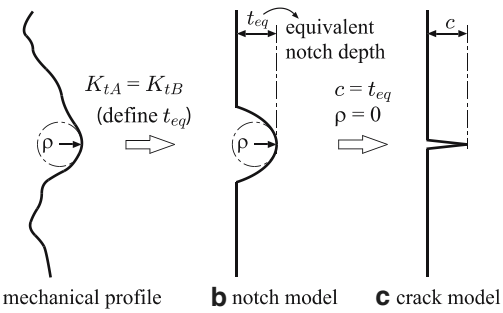

Fig. 2 Evaluation of notch depth and crack length

When $\rho \le \rho_0$, the macrocrack arrests under the notch root and the non-propagating macrocrack limit σ_{w2} becomes the fatigue limit. Because the fatigue limit of the notched specimen with ρ and t_{eq}, σ_{w2}, is independent of ρ, and equals to the fatigue limit of the cracked specimen with $\rho = 0$ and the crack depth $c = t_{eq}$, the notch can be considered as a crack with $c = t_{eq}$ mechanically.

The σ_{w1} is predicted by Eqs. (1) and (2). The σ_{w2} is predicted by Eqs. (3) and (4). Because there is a competitive relation between the σ_{w1} and σ_{w2}, the fatigue limit of the mechanical profile, σ_w, is obtained from Eq. (5). So, even if the surface roughness is significantly complex, the surface is coarse-grained and its fatigue limit can be predicted by the unit notch or crack model.

4 Approximate method for calculation of stress concentration factor of mechanical profile

It is supposed that strength of the mechanical profile obeys the weakest link model (Weibull 1951). The con-

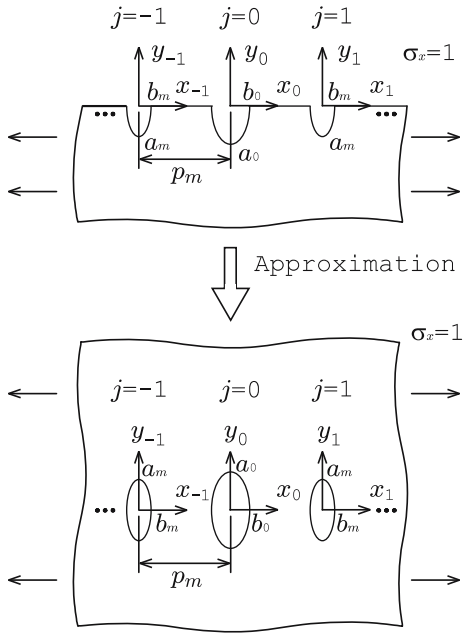

Fig. 3 Schematic illustrations of infinite parallel rows of elliptical holes in an infinite plate and elliptical notches in a semi-infinite plate

cavities and convexities in the mechanical profile are divided into the severest notch and the other notches. Because the mechanical profile is significantly complex, the complex stress distributions are each formed under all of the notch roots. However, the local stress concentration in a position away from the notch root is reduced according to the Saint-Venant's principle, the factor which governs the stress distribution changes from the local notch shape to the average one.

From the above reasoning, in this study, the mechanical profile is expressed with "the local notch" and a parallel row of "the average notches". Then, as shown in Fig. 3, the SCF of the mechanical profile is evaluated by approximating the notches in the semi-infinite plate with elliptical holes in an infinite plate. In Fig. 3, the 0-th hole corresponds to the local notch, where a_0 is a semi-major axis, b_0 a semi-minor axis, $\rho_0 = b_0^2/a_0$ a notch root radius, $t_0 = a_0$ a notch depth. And then, the $j(= \pm 1, \pm 2, \cdots)$-th holes correspond to the average notches, where a_m is a semi-major axis, b_m a semi-minor axis, $\rho_m = b_m^2/a_m$ a notch root radius, $t_m = a_m$ a notch depth. p_m is an average interval between the notches.

4.1 Transformation from mechanical profile to infinite parallel row of notches

When there are $(2N + 1)$ concavities and convexities which can be treated as the notchs in the mechanical profile, the method for evaluating, the interval p_m, a notch depth t_m and a notch root radius ρ_m of the average notch, a notch depth t_0 and a notch root radius ρ_0 of the local notch from the mechanical profile is mentioned in this section.

4.1.1 Evaluation of p_m

The mechanical profile $W(x)$, which is obtained by removing the high frequency profiles from the mechanical profile so as to meet Eq. (8), is expressed by a Fourier series.

$$W(x) = \sum_{n=0}^{\infty} c_n(f_n)\, e^{i2\pi f_n x} \tag{9}$$

$$c_n(f_n) = \frac{1}{L} \int_{-L/2}^{L/2} W(x)\, e^{-i2\pi f_n x} dx \tag{10}$$

Here, L is the distance from the beginning of the roughness profile to the end and a constant which is obtained when the profile is measured, $f_n = n/L$. The frequency where the spectrum becomes a maximum is denoted with f_m. It is supposed that the reciprocal f_m is p_m $(= 1/f_m)$.

4.1.2 Evaluations of ρ_0 and ρ_m

The x coordinate under the j-th notch root on the $W(x)$ is denoted with x_j. The j-th notch root radius at x_j, ρ_j, is expressed with the following equation.

$$\frac{1}{\rho_j} = \frac{\left| \frac{d^2 W(x)}{dx^2} \Big|_{x=x_j} \right|}{\left\{ 1 + \left(\frac{dW(x)}{dx} \Big|_{x=x_j} \right)^2 \right\}^{3/2}} \tag{11}$$

Because the 0-th notch is the local notch, the average of all notch root radii except for ρ_0 is adopted as the average notch root radius ρ_m.

4.1.3 Evaluations of t_0 and t_m

The frequencies of $W(x)$ are divided into f_m and other frequencies. The former forms a periodic profile with a

period p_m, the latter gives the periodic profile irregularity. When the profile with p_m is denoted with $W_m(x)$, the $W_m(x)$ corresponds to the infinite parallel row of the average notches.

When several similar notches are arranged, regions where shear stress $\tau_{xy} = 0$ and which are not related to a stress distribution form between the notches (Neuber 1958). Therefore, when the parallel row of the notches is approximated with that of the elliptical holes, the distance from the boundary of the region to the notch root has to be used as the semi-major axis of the hole. The distance is called the effective notch depth t_{eff}. Figure 4 shows a schematic illustration of a relation between the mechanical profile and the parallel notch model. When t_m^*, which is the average of t_j $(j = \pm 1, \ldots, \pm N)$, p_m and ρ_m are used as the parameters, the parallel row of notches in $W(x)$ is approximated with that of average notches through an arbitrary periodical profile $W_m^*(x)$ whose parameters equal those of $W(x)$. Finally, the notches in the semi-infinite plate are approximated with the elliptical holes in the infinite plate. The notch depth of the elliptical notch is denoted with $t_m (= t_{\text{eff}})$.

The height from standard $W(x) = 0$ to the highest peak of $W_m(x)$ is used as the height from the standard to a free surface. The notch depth of the j-th notch, t_j, is expressed with the following equation.

$$t_j = \max\left(W_m(x)\right) - W(x_j) \tag{12}$$

The notch depth of $W_m^*(x)$, t_m, is chosen so that the SCF of $W_m^*(x)$ equals that of the infinite parallel row of the semi-elliptical notches with ρ_m. The t_m is expressed with the following equation.

$$t_m = K_{tm}^{-1}(p_m, \rho_m, t_m)|_{K_{tm}=K_{tm}^*} \tag{13}$$

Here, $K_{tm}(p_m, \rho_m, t_m)$ is the SCF of the infinite parallel row of the average notches, K_{tm}^* is the SCF of $W_m^*(x)$, and $K_{tm}^{-1}(p_m, \rho_m, t_m)|_{K_{tm}=K_{tm}^*}$ is a function which is obtained by solving $K_{tm}(p_m, \rho_m, t_m) = K_{tm}^*$ on the notch depth t_m.

The distance from the standard $W(x) = 0$ to the j-th notch root is expressed with $-W(x_j)$. Therefore, an average height from the standard to the free surface is obtained as follows by subtracting an average of all distances from the t_m.

$$t_m - \frac{1}{2N}\sum_{\substack{-N \\ j\neq 0}}^{N}\left\{-W(x_j)\right\} \tag{14}$$

Therefore, the local notch depth t_0 is obtained by adding the distance from the standard to the 0-th notch root,

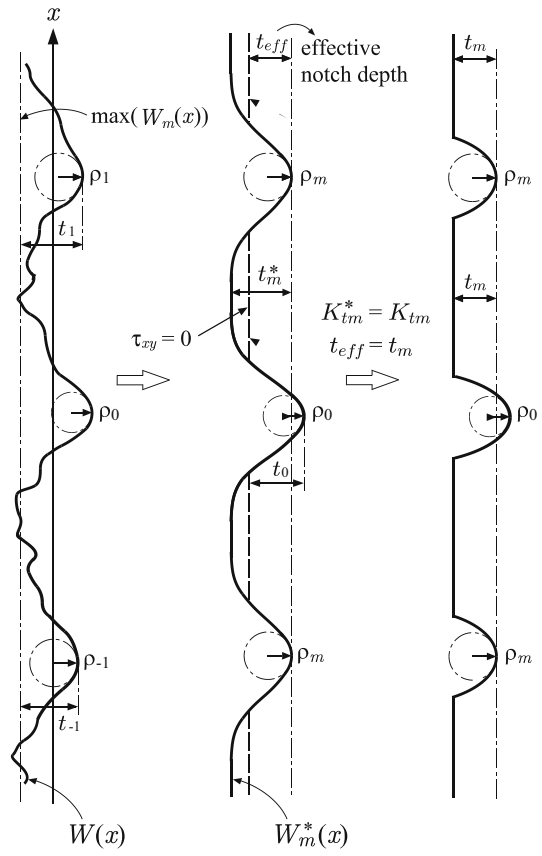

Fig. 4 Schematic illustration of a relation between mechanical profile and parallel notch model

$-W(x_0)$, to Eq. (14) as follows.

$$t_0 = t_m + \frac{1}{2N}\sum_{\substack{-N \\ j\neq 0}}^{N} W(x_j) - W(x_0) \tag{15}$$

4.2 Stress concentration factor at the local notch

When there are several notches, the stress field of one notch is disturbed by the other notches. The interference problem is caused by such disturbances of the stress fields must be determined (Nisitani 1968; Nisitani 1978). In this section, the method to determine the unknown stress field is described.

Let us consider the tensile problem of the infinite plate with the parallel row of elliptical holes under the applied stresses $\sigma_{x\infty} = 1$ and $\sigma_{y\infty} = 0$. When the interference problem is replaced with the tensile problem of the single k-th hole in the infinite plate, the applied stress to the

k-th hole, $\sigma_{x\infty} = X_k$, is expressed with the following equation (Nisitani 1968; Nisitani 1978).

$$X_k = 1 + \sum_{\substack{j=-\infty \\ j\neq k}}^{\infty} \sigma_{xj}(X_j, 0)\Big|_{\substack{x_j=(k-j)p_m \\ y_j=-a_k}} \tag{16}$$

Here, $\sigma_{xj}(\sigma_{x\infty}, \sigma_{y\infty})$ is an additional stress in a point (x_j, y_j) by the j-th hole in the infinite plate under $\sigma_{x\infty}$ and $\sigma_{y\infty}$ (see Appendix A).

In this paper, it is supposed that a metal is surface-finished by a turning machine, grinding machine, emery paper, etc. and its surface does not have extreme sharp and deep notches. Therefore, because the shapes and sizes of the convexities and concavities are comparable although they each vary randomly, the difference between the local and average notches is assumed to be little. The notch interference problem is solved approximately based on the following assumption (the application limit of the approximation is mentioned in Sect. 5).

$$X_j = \begin{cases} X_0 & (j = 0) \\ X_m & (j = \pm 1, \ldots, \pm\infty) \end{cases} \tag{17}$$

First, let us consider that the stress X_0 which is applied to the 0-th elliptical hole. Substituting $k = 0$ and $X_j = X_m$ $(j = \pm 1, \ldots, \pm\infty)$ into Eq. (16), the following equation is obtained.

$$X_0 + \delta X_0 = 1 + X_m \sum_{\substack{j=-\infty \\ j\neq 0}}^{\infty} \sigma_{xm}(1, 0)\Big|_{\substack{x_j=-jp_m \\ y_j=-a_0}} \tag{18}$$

Here, $\sigma_{xm}(1, 0) = \sigma_{xj}(1, 0)$ $(j = \pm 1, \ldots, \pm\infty)$, δX is the error due to the approximation. When $X_0 = X_m$, the local notch becomes equal to the average notch and X_0 is expressed with the following equation.

$$X_0 = X_m = \frac{K_{tm}}{K_{tm}|_{p_m=\infty}} \tag{19}$$

Here, K_{tm} is the SCF of the semi-infinite plate with an infinite parallel row of average notches under the tensile stress (see Appendix B). When δX_0 is decided to satisfy Eq. (19), it is given by the following equation.

$$\delta X_0 = 1 - \frac{K_{tm}}{K_{tm}|_{p_m=\infty}} \left\{ 1 - \sum_{\substack{j=-\infty \\ j\neq 0}}^{\infty} \sigma_{xm}(1, 0)\Big|_{\substack{x_j=-jp_m \\ y_j=-a_m}} \right\} \tag{20}$$

Finally, substituting Eq. (20) into Eq. (18), X_0 is obtained as follows.

$$X_0 - X_m \sum_{\substack{j=-\infty \\ j\neq 0}}^{\infty} \sigma_{xm}(1, 0)\Big|_{\substack{x_j=-jp_m \\ y_j=-a_0}} = \frac{K_{tm}}{K_{tm}|_{p_m=\infty}} \left\{ 1 - \sum_{\substack{j=-\infty \\ j\neq 0}}^{\infty} \sigma_{xm}(1, 0)\Big|_{\substack{x_j=-jp_m \\ y_j=-a_m}} \right\} \tag{21}$$

Next, let us consider the first hole and its applied stress X_m. Substituting $k = 1$ and Eq. (17) into Eq. (16), X_m is obtained as follows.

$$X_m + \delta X_m = 1 + X_m \sum_{\substack{j=-\infty \\ j\neq 1}}^{\infty} \sigma_{xm}(1, 0)\Big|_{\substack{x_j=(1-j)p_m \\ y_j=-a_m}} - X_m \sigma_{xm}(1, 0)\Big|_{\substack{x_0=p_m \\ y_0=-a_m}} + X_0 \sigma_{x0}(1, 0)\Big|_{\substack{x_0=p_m \\ y_0=-a_m}} \tag{22}$$

Here, δX_m is an error due to the approximation. The right hand side of Eq. (22) means an elliptical hole is taken out from the infinite parallel row of the average holes with semi-major axis a_m and semi-minor axis b_m and it is replaced by a local elliptical hole with semi-major axis a_0 and semi-minor axis b_0. Because the second term of the right hand side of Eq. (22) means a summation of additional stresses by the infinite parallel row of the average notches, the following equation is obtained from Eq. (19).

$$\sum_{\substack{j=-\infty \\ j\neq 1}}^{\infty} \sigma_{xm}(1, 0)\Big|_{\substack{x_j=(1-j)p_m \\ y_j=-a_m}} = 1 - \frac{K_{tm}}{K_{tm}|_{p_m=\infty}} \tag{23}$$

Substituting Eq. (23) into Eq. (22) and deciding δX_m to satisfy Eq. (19), δX_m is obtained as follows.

$$\delta X_m = 0 \tag{24}$$

Substituting Eqs. (23) and (24) into Eq. (22), X_m is obtained as follows.

$$X_m = 1 + X_m \left\{ \left(1 - \frac{K_{tm}}{K_{tm}|_{p_m=\infty}} \right) - \sigma_{xm}(1, 0)\Big|_{\substack{x_0=p_m \\ y_0=-a_m}} \right\} + X_0\, \sigma_{x0}(1, 0)\Big|_{\substack{x_0=p_m \\ y_0=-a_m}} \tag{25}$$

Moreover, by rearranging terms of Eq. (25), the following equation is obtained.

$$\left\{ \frac{K_{tm}}{K_{tm}|_{p_m=\infty}} + \sigma_{xm}(1, 0)\Big|_{\substack{x_0=p_m \\ y_0=-a_m}} \right\} X_m - X_0 \sigma_{x0}(1, 0)\Big|_{\substack{x_0=p_m \\ y_0=-a_m}} = 1 \tag{26}$$

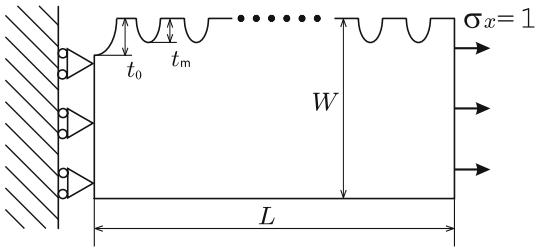

Fig. 5 Schematic illustration of a model analyzed by FEM

Finally, solving simultaneous equations of Eqs. (21) and (26), X_0 and X_m are obtained. The SCF of the local notch, K_{t0}, is obtained from the following equation.

$$K_{t0} = K_{t0}|_{p_m=\infty} X_0 \tag{27}$$

Here, $K_{t0}|_{p_m=\infty} = 1 + 2\sqrt{t_0/\rho_0}$.

5 Application limit of approximate calculation method

In this section, the limit of application of the method presented in Sect. 4 is examined using the analysis models which are constituted by the local notch and the average notches.

5.1 FEM analysis and boundary condition

Figure 5 shows a schematic illustration of an analysis model. The FEM analyses were carried out changing the number of the element division and length L, width W of the finite plate based on the notch depth t_m so that the analyzed result was independent of the model and the element division. The ratios of W and L to t_0 were $W/t_0 \simeq 100$ and $L/t_0 \simeq 200$, respectively.

5.2 Examination of application limit

Under the pre-condition of Appendix C, the analyses were carried out changing the sizes, shapes and periods of the notchs like $\sqrt{t_m/\rho_m} = \sqrt{t_0/\rho_0} = 1, 2, 4$ and $p_m/t_m = 2.5, 3, 4$. Figure 6 shows results of comparison between $K_{t0}|_{\text{present}}$ by the present method and $K_{t0}|_{\text{FEM}}$ by the FEM analysis. For $t_0/t_m \simeq 1$, because $K_{t0}|_{\text{present}}$ is governed by the accuracy of Eq. (45), the smaller $\sqrt{t_m/\rho_m}$ is, the closer the $K_{t0}|_{\text{present}}/K_{t0}|_{\text{FEM}}$ comes to 1. From Fig. 6, when the local notch, similar to the average one, satisfies the following conditions, then the SCF can be predicted to within ±5% error.

$$1.0 \le t_0/t_m \le 1.2 \tag{28}$$

$$2.5 \le p_m/t_m \le 4.0 \tag{29}$$

$$2.0 \le \sqrt{t_m/\rho_m} \le 4.0 \tag{30}$$

Figure 7 shows the $K_{t0}|_{\text{present}}/K_{t0}|_{\text{FEM}}$ values which were calculated changing $\sqrt{t_0/\rho_0}$ under $t_0/t_m = 1.2$, $\sqrt{t_m/\rho_m} = 2, 4$. From Fig. 7, when the local notch is not similar to the average one and satisfied with the following conditions, the SCF can be predicted within ± 5% error.

$$1.0 \le \sqrt{\frac{t_0}{\rho_0}} \Big/ \sqrt{\frac{t_m}{\rho_m}} \le 2.0 \tag{31}$$

Therefore, when the notches are satisfied with Eqs. (28), (29), (30) and (31), the stress concentration factor can be predicted within ± 5% error.

The real surface roughness is different from the parallel row of notches geometrically. However, the stress by the notch is governed by the ρ and t. When ρ_0, t_0, ρ_m, t_m and p_m are chosen appropriately, it seems that the real surface roughness can be simulated by the parallel row of notches and Eqs. (28), (29), (30) and (31) are approximately useful.

6 Examination of application limit

In this section, the validity of the present method and its application limit in Sect. 5 is examined using a finite parallel row of notches with various shapes and periods and real surface roughness (Aono and Noguchi 2004).

6.1 profile of the infinite parallel row of semi elliptical holes

In order to examine the validity of the present method and its application limit, the numerical simulations were carried out on three kinds of simple models with the parallel row of various elliptical notches. The local notch depth t_0 was set at 1.2. Then, the p_m/t_m and t_0/t_m of the models were determined by referring to those of the real surface roughness. The shapes and intervals of the notches were varied randomly within a range of $t_j \pm \delta t_j$, $p_j \pm \delta p_j$ and $\sqrt{t_j/\rho_j} \pm \delta\sqrt{t_j/\rho_j}$. Table 1 shows the parameters of the models. The parameters

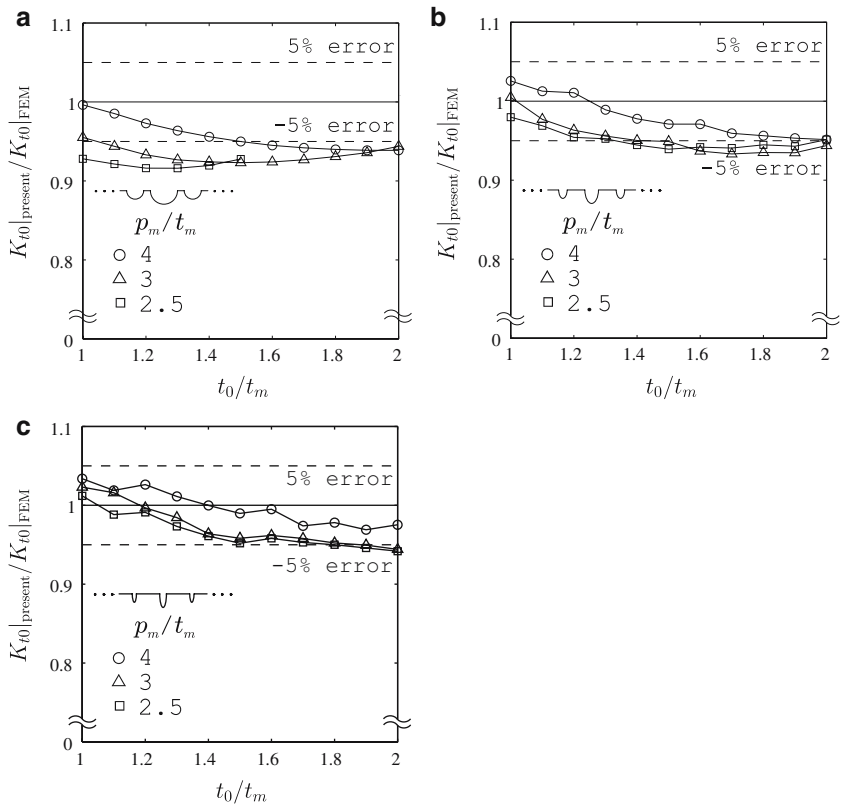

Fig. 6 Relation between $K_{t0}|_{present}/K_{t0}|_{FEM}$ and t_0/t_m
(a) $\sqrt{\rho_0/t_0} = \sqrt{\rho_m/t_m} = 1$
(b) $\sqrt{\rho_0/t_0} = \sqrt{\rho_m/t_m} = 2$
(c) $\sqrt{\rho_0/t_0} = \sqrt{\rho_m/t} = 4$

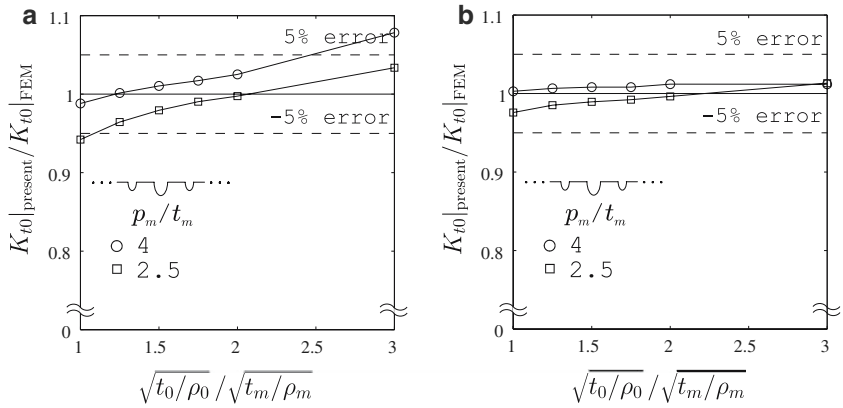

Fig. 7 Relation between $K_{t0}|_{present}/K_{t0}|_{FEM}$ and $\sqrt{t_0/\rho_0}/\sqrt{t_m/\rho_m}$ under $t_0/t_m = 1.2$ (a)
$\sqrt{t_m/\rho_m} = 2$ (b)
$\sqrt{t_m/\rho_m} = 4$

were determined referring to the those of the real surface roughness. For example, the t_0/t_m and p_m/t_m of the models are similar to those of the real roughness in the following Sect. 6.2; the p_m/t_m values of the models and the real roughness ranges from 2.61 to 3.64 and from 3.14 to 3.33, respectively; the t_0/t_m values of the models and the real roughness ranges from 1.0 to 1.09 and from 0.9 to 1.38, respectively.

Table 1 Parameters of notch configurations

	t_0	$\sqrt{\frac{t_0}{\rho_0}}$	$t_j \pm \delta t_j$	$\sqrt{\frac{t_j}{\rho_j}} + \delta\left(\sqrt{\frac{t_j}{\rho_j}}\right)$	$p_j + \delta p_j$
Model I	1.2	2.5	1.0 ± 0.15	2.09 ± 0.32	2.59 ± 0.72
Model II	1.2	4.0	1.1 ± 0.05	3.00 ± 0.95	3.18 ± 0.80
Model III	1.2	6.0	1.1 ± 0.10	3.45 ± 0.71	4.09 ± 0.69

$j = \pm 1, \pm 2, \ldots, \pm N$ ($2N$ is the number of average notches.)

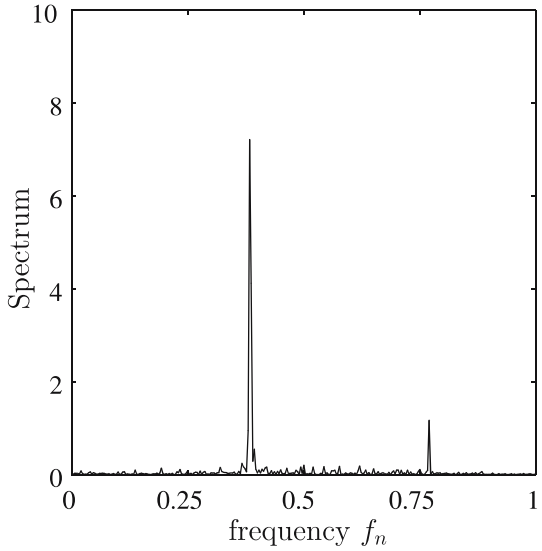

Fig. 8 Spectrum of simulated surface roughness of model I

6.1.1 FEM analysis and boundary condition

Because notches which have various ρ and t were arranged randomly, asymmetrical models $2W$ in width and L in height were analyzed. The ratios of W and L to t_0 were $W/t_0 \simeq 100$ and $L/t_0 \simeq 200$, respectively.

6.1.2 comparison between calculated and analyzed results

ρ_0, t_0, ρ_m, t_m and p_m are determined according to Sect. 4.1. Because the analyzed model is the parallel row of elliptical notches, the distance from the surface to the notch root is used as the notch depth t_j. Figure 8 shows the relation between the power spectrum and frequency. Table 2 shows t_m, $\sqrt{t_m/\rho_m}$, p_m, K_t due to the present method and FEM analysis. Comparing $K_t|_{\text{present}}$ with $K_t|_{\text{FEM}}$, all of the K_t values are within about 10 % error.

6.2 profile of real surface roughness

In this section, the validity of the present method and its application limit were examined by using the real surface roughness of 0.1% carbon steel. The roughness was machined under the condition of 0.15 mm depth of cut and manual feed by a turning machine (Aono and Noguchi 2004).

Figure 9(a) shows the analyzed profiles. The solid line is a mechanical profile; the chained line is the Hirano's conformal mapping function which gives the best fit for the mechanical profile (Aono and Noguchi 2004). For the fitting profile, the notch depths of the notch model, t_j, range from 55.4 μm to 98.5 μm. The notch radii of the notch model, ρ_j, range from 15.0 μm to 57.0 μm. Figure 9(b) shows a spectrum of the mechanical profile. In this analysis, the K_t values at $x_j = 57, 784, 1233\,\mu$m in the mechanical profile and $x_j = 70, 744, 1229\,\mu$m in the fitting profile were each calculated. Table 3 shows the ρ_0, t_0, ρ_m and t_m of the profiles, respectively. The parameters were determined from the t_j and ρ_j values according to Sect. 4.1. Also, because the spectrum of the mechanical profiles has peaks at $f_n = 1/2381, 3/2381, 6/2381$, the p_m was assumed to be $2381/10 \simeq 238\,\mu$m. The present notch model which was used in the process of calculating the K_t at $x = 1229\,\mu$m was added as the broken line in Fig. 9(a).

Figure 9(c) shows K_t and $\sigma_1/\sigma_{x\infty}$ of the profiles in Fig. 9(a). The solid line is the $\sigma_1/\sigma_{x\infty}$ distribution of the mechanical profile which was calculated by the complex variable method using Hirano's conformal mapping function; the open circle and triangle marks are the K_t values of the mechanical profile and the fitting profile which were calculated by the present method, respectively. The locations of the notch roots in the broken line roughly corresponds to those in the solid line in Fig. 9(a). Additionally, eight local maximum values are also found in the solid line macroscopically. Because the peaks mean that eight main notches exist

Table 2 Exact and present solutions

	t_m	$\sqrt{\frac{t_m}{\rho_m}}$	p_m	$K_t\|_{\text{present}}$	$K_t\|_{\text{FEM}}$
Model I	1.00	2.00	2.61	3.96	4.02
Model II	1.10	2.68	3.26	6.23	6.51
Model III	1.10	3.24	4.00	10.00	9.84

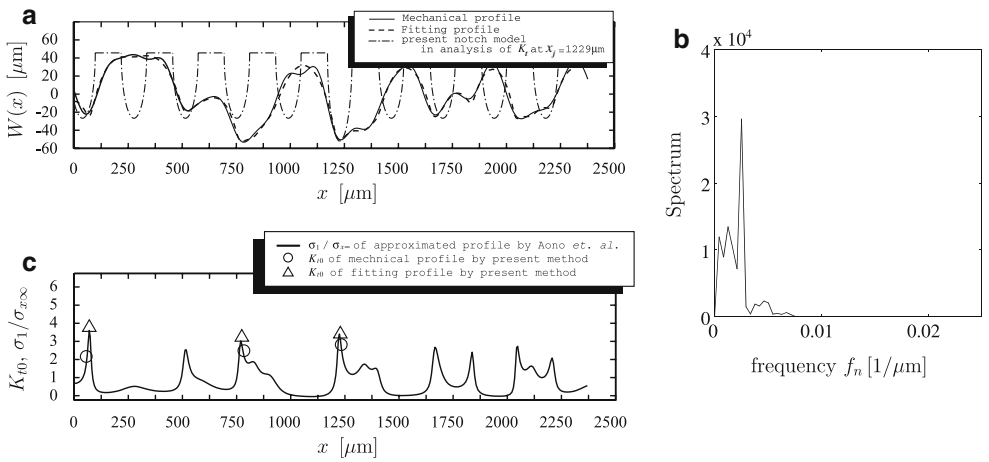

Fig. 9 Simulated model and results of complex surface roughness (a) Mechanical profile and approximated profile (b) Spectrum analysis (c) Stress concentration factor and equivalent stress distribution

Table 3 Parameters of notch configurations

j	x_j	ρ_0	t_0	ρ_m	t_m	$\frac{p_m}{t_m}$	$\frac{t_0}{t_m}$	$\sqrt{\frac{t_0}{\rho_0}}$	$\sqrt{\frac{t_m}{\rho_m}}$
1	56	48.5	67.9	71.1	75.9	3.14	0.90	1.18	1.03
	(70)	(15.0)	(69.7)	(43.1)	(75.8)	(3.14)	(0.92)	(2.15)	(1.33)
2	784	69.6	98.7	68.1	71.5	3.33	1.38	1.19	1.02
	(744)	(38.6)	(98.5)	(40.2)	(72.2)	(3.30)	(1.36)	(1.60)	(1.34)
3	1233	49.3	97.9	71.0	71.8	3.31	1.36	1.41	1.01
	(1229)	(33.3)	(97.3)	(40.8)	(72.3)	(3.29)	(1.35)	(1.71)	(1.33)

(x_j, ρ_0, t_0, ρ_m, t_m:μm)

in the mechanical profile of $L = 2381\,\mu$m, the validity of $p_m = 238\,\mu$m is confirmed. When the $\sigma_1/\sigma_{x\infty}$ distribution corresponds to the fitting profile in Fig. 9(a), all peaks on the $\sigma_1/\sigma_{x\infty}$ distribution occur at the notch roots and the direction of the local maximum values of the σ_1 corresponds to that of the $\sigma_{x\infty}$.

Comparing the triangle marks to the solid line, both of them correspond well. The K_t predicted by the present method basically contain errors which are caused by two differences: the difference between the complex profile and the parallel row of elliptical notches; the difference between the simple model with various notches and the present model with average notches and the local notch. The former is confirmed by comparing the square marks to the solid line. On the other hand, the latter is roughly estimated by Table 3 and the application limit of Eqs. (28), (29), (30) and (31). Comparing the solid line with the circle marks, there are the large errors between them. The errors are caused by the difference between the real surface roughness and the fitting profile in addition to the errors due to the above differences.

Conclusively, if the concavities and convexities are distributed randomly even if the profile is complex, the surface roughness can be approximated with the infinite parallel row of elliptical notches and its K_t can be approximately predicted by the present model with the average notches and the local notch.

7 Conclusion

In order to predict the fatigue limit of a specimen with a two dimensional complex surface, a practical method to estimate a SCF of its surface roughness was proposed. The conclusions of the present study are summarized as follows.

1. The practical method to evaluate the SCF by replacing the surface roughness with a parallel row of the local notch and innumerable average notches was proposed. Then, an approximate method to calculate the SCF by replacing the notches with an elliptical hole and superposing the elastic solution of the holes was proposed as in Eqs. (21), (26) and (27).
2. The FEM analyses were carried out on several models, changing the shapes and sizes of the local notch and the average notches. The application limit was examined and obtained as Eqs. (28), (29), (30) and (31).
3. The validity of the application limit was examined by using the real roughness and the infinite parallel row of various notches.

Appendix

A The additional stress due to the elliptical hole at a point

Let us consider a tensile problem of an infinite plate with an elliptical hole. The origin is set to the center of the hole. Then, the major axis and minor axis are set to a in x axis and b ($< a$) in y axis, respectively. The stress which is added by the elliptical hole at $z = x + iy$ is expressed as follows (Nisitani 1968).

$$\sigma_x^* = \mathrm{Re}\Big[-A\left\{\frac{2\,e^{-\zeta}}{\sinh\zeta} + \frac{\cosh\bar{\zeta}}{\sinh^3\zeta}\right\} + B\,\frac{\cosh\zeta}{\sinh^3\zeta} - 2\,C\,\frac{(2\,\sinh\zeta + \cosh\zeta)\,e^{-2\zeta}}{\sinh^3\zeta}\Big] \tag{32}$$

$$\sigma_y^* = \mathrm{Re}\Big[-A\left\{\frac{2\,e^{-\zeta}}{\sinh\zeta} - \frac{\cosh\bar{\zeta}}{\sinh^3\zeta}\right\} - B\,\frac{\cosh\zeta}{\sinh^3\zeta} + 2\,C\,\frac{(2\,\sinh\zeta + \cosh\zeta)\,e^{-2\zeta}}{\sinh^3\zeta}\Big] \tag{33}$$

$$\tau_{xy}^* = \mathrm{Im}\Big[A\,\frac{\cosh\bar{\zeta}}{\sinh^3\zeta} - B\,\frac{\cosh\zeta}{\sinh^3\zeta} + 2\,C\,\frac{(2\,\sinh\zeta + \cosh\zeta)\,e^{-2\zeta}}{\sinh^3\zeta}\Big] \tag{34}$$

Here, A, B and C are constants which depend on the boundary condition, $z - \sqrt{a^2 - b^2}\cosh\zeta$, $\zeta = \xi + i\eta$, $i = \sqrt{-1}$. When the boundary condition is $\sigma_{y\infty} = 1$ and $\sigma_{x\infty} = \tau_{xy\infty} = 0$, A, B and C are given as follows.

$$A = -\frac{1}{2\,(1-\varepsilon)} \tag{35}$$

$$B = -\frac{1}{2\,(1-\varepsilon^2)} \tag{36}$$

$$C = \frac{\varepsilon}{4\,(1-\varepsilon)^2} \tag{37}$$

Here, $\varepsilon = b/a$.

When $\sigma_{x\infty} = X_j$ and $\sigma_{y\infty} = 0$ are applied to the infinite plate with only the j-th elliptical hole, the stress which is added at the point (x_j, y_j) by the hole is obtained by substituting Eqs. (35), (36) and (37) into Eq. (33), considering the direction of the semi-major and semi-minor axes in Eqs. (35), (36) and (37).

$$\sigma_{xj}(X_j, 0) = X_j\,\sigma_y^*\big|_{z=y_j+ix_j} \tag{38}$$

B Derivation of approximate formulae of $K_{tm}|_{p=\infty}$ and K_{tm}

The SCF of the elliptical hole in the infinite plate under the tensile stress $\sigma_{x\infty} = 1$ is given by the following equation.

$$K_t = 1 + 2\sqrt{\frac{a}{\rho}} \tag{39}$$

Here, ρ is a notch root radius, a is a semi-major axis. Moreover, the SCF of the infinite parallel row of notches with a period p_m in the semi-infinite plate under $\sigma_{x\infty}$ is denoted with K_{tm}. $K_{tm}|_{p=\infty}$, which corresponds to the SCF of the unit notch in a semi-infinite plate, is expressed with the following equation.

$$K_{tm}|_{p=\infty} = F_t \cdot K_t \tag{40}$$

Here, F_t is a modified parameter of the elliptical notch to the elliptical hole with the semi-major axis a and notch root radius ρ in the infinite plate under the tensile stress. In this paper, the following equation is used as an approximate formula (Noda et al. 1997).

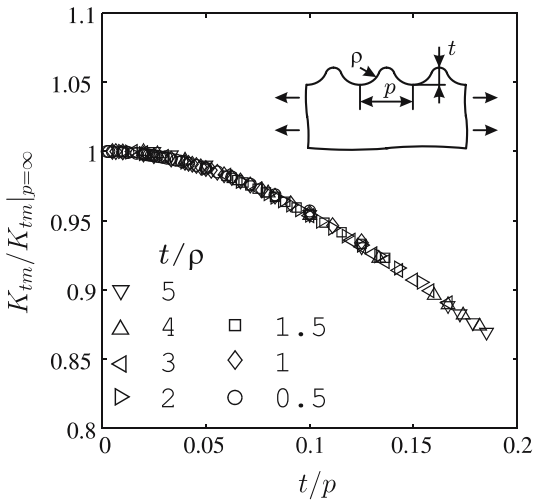

Fig. 10 Relation between K_{tm}/K_{t0} and t/p

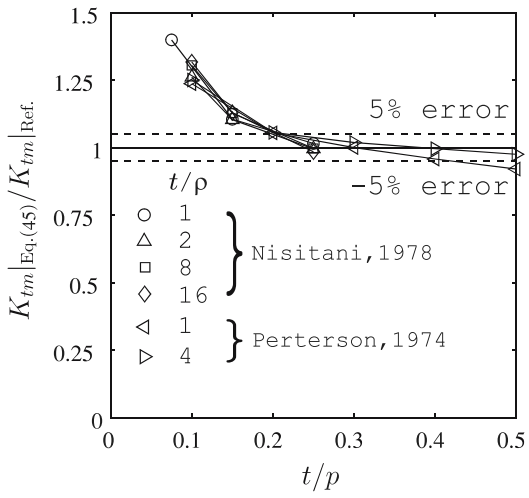

Fig. 11 Relation between $K_{tm}|_{\mathrm{Eq.\,(45)}}/K_{tm}|_{\mathrm{Ref.}}$ and t/p

$$F_t = 1.148 - 0.160\left(\frac{\rho}{a}\right)^{1/2} - 0.0345\left(\frac{\rho}{a}\right) + 0.0693\left(\frac{\rho}{a}\right)^{3/2} \tag{41}$$

The stress intensity factor of edge cracks which constitute the parallel infinite row in a semi-infinite plate is denoted with K_{Im}. The K_{Im} is independent of the crack length t and expressed with the following equation by J integral (Rice 1968).

$$K_{Im} = \sigma_{x\infty}\sqrt{\frac{p}{2}} \tag{42}$$

On the other hand, when $p = \infty$, $K_{Im}|_{p=\infty}$ is equal to the stress intensity factor of the edge crack with the crack length t in the semi-infinite plate and given by the following equation.

$$K_{Im}|_{p=\infty} = 1.121\,\sigma_{x\infty}\sqrt{\pi\, t} \tag{43}$$

Figure 10 shows the K_{tm} values calculated by the previous method (Aono and Noguchi 2004) against the various t/ρ and t/p. From this figure, the K_{tm} is independent of t/ρ and expressed with the function of only t/ρ. Also, because the crack corresponds to the notch with $\rho \to 0$, $K_{tm}/K_{tm}|_{p=\infty}$ is approximated by the following equation.

$$\frac{K_{tm}}{K_{tm}|_{p=\infty}} \simeq \frac{K_{Im}}{K_{Im}|_{p=\infty}} \tag{44}$$

Substitiuting Eqs. (40), (42) and (43) to Eq. (44) and solving on K_{tm}, the following equation is obtained.

$$K_{tm} = \frac{F_t}{1.121\sqrt{2\,\pi}}\left(\sqrt{\frac{p}{t}} + 2\sqrt{\frac{p}{\rho}}\right) \tag{45}$$

When $p, \rho \ll t$, Eq. (45) is approximated with the following equation.

$$K_{tm} \simeq \sqrt{\frac{2\,p}{\pi\rho}} \tag{46}$$

C Accuracy of Eq. (45)

Figure 11 shows a result of a comparison of the K_t values of various notches by Eq. (45) and References (Peterson 1974; Nisitani 1978). From this figure, when the notch is satisfied with the following equations, the SCF can be predicted within ± 5% error.

$$2.5 \le p_m/t_m \le 4.0 \tag{47}$$

$$1 \le \sqrt{t_m/\rho_m} \le 4 \tag{48}$$

Because Eq. (45) is derived based on Eq. (44), the smaller the p and ρ are, the more accurate Eq. (45) becomes.

Figure 12 shows the K_{tm} values by Eq. (45) and References (Peterson 1974; Nisitani 1978) against t_m/p. From this figure it is found that the K_{tm} values are independent of t_m/ρ_m and expressed with a function of p/ρ_m, when ρ_m, $p \ll t_m$.

In this paper, Eq. (45) was used to give priority to simplicity and convenience. If the exact solution is used instead of Eq. (45), the accuracy and application limit of the present method will improve.

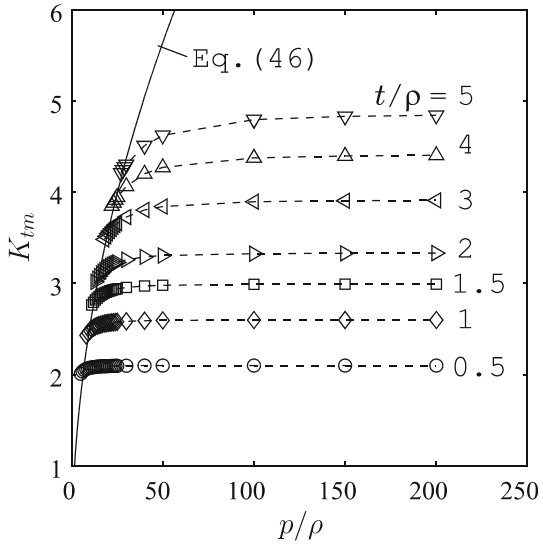

Fig. 12 Relation between K_{tm} and p/ρ

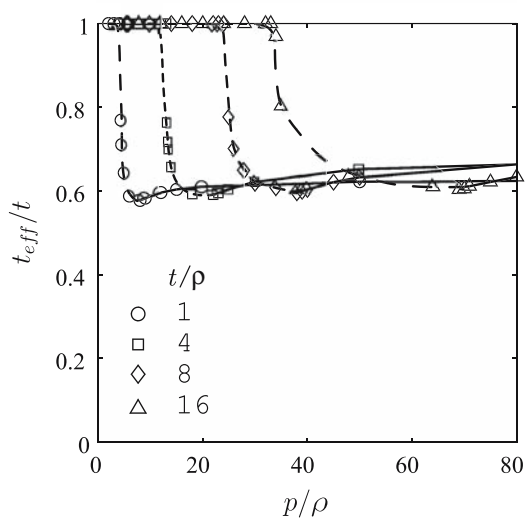

Fig. 13 Relation between t_{eff}/t and p/ρ

D The effective notch depth of the profile due to Hirano's conformal mapping function

Hirano's conformal mapping function was used as $W_m^*(x)$, and t_{eff} is calculated by solving Eq. (13) numerically using FEM. Figure 13 shows a relation between t_{eff}/t and p/ρ using t/ρ as a parameter. However, because it is difficult to form the profile by Hirano's conformal mapping function and the K_{tm}^* cannot be calculated when p/ρ becomes smaller than the critical value, the K_{tm}^* values which are extrapolated by the obtained K_{tm}^* value are used. The broken lines in Fig. 13 are the K_{tm}^* values by the extrapolated values. When p/ρ becomes small, the extrapolated K_{tm}^* value becomes close to K_{tm} and $t_{\text{eff}} = 1$. On the other hand, when the p/ρ becomes large, $t_{\text{eff}} = 0.65$ independent of t/ρ.

References

Aono Y, Noguchi H (2004) Fatigue limit reliability of axisymmetric complex surface. Int J Fract 131(1): 59–78

Hirano F (1950) Study on the Shape Facture of 2D Elastic Body. J Jpn Soc Mech Engineers (in Japanese) 16(55): 52–58

Isibasi T (1954) Prevention of fatigue and fracture of metals, (in Japanese), Yokendo

Miyazaki T, Noguchi H, Ogi K (2004) Quantitative evaluation of fatigue limit of a metal with an arbitrary crack under a Stress Controlled Condition (Stress ratio = −1). Int J Fract 129(1): L21–L38

Murakami Y (2002) Metal fatigue: effects of small defects and nonmetallic inclusions. Elsevier

Murakami Y, Tsutsumi K, Fujishima M (1996) Quantitative evaluation of the effect of surface roughness on fatigue strength. Trans Jpn Soc Mech Engineers (in Japanese), 62–597(A): 1124–1131

Murakami Y, Takahashi K, Yamashita T (1997) Quantitative evaluation of the effect of surface roughness on fatigue strength (effect of depth and pitch of roughness). Trans Jpn Soc Mech Engineers, (in Japanese), 63–612(A): 1612–1619

Neuber H (1958) Kerbspannungslehre. Springer-Verlag, Berlin

Nishihara T, Fujii T (1951) Stress in a semi-infinite plate having manyfold notches. J Jpn Soc Mech Engineers, (in Japanese), 17–61: 6–12

Nisitani H (1968) Method of approximate calculation for interference of notch effects and its application. Bull JSME 11(47): 725–738

Nisitani H (1972) Correlatoin between notch sensitivity of a material and its non-propagating crack under rotating bending stress. Proceedings of the 1971 International Conference on Mechanical Behavior of Materials II(47): 312–322

Nisitani H (1978) Solution of notch problems by body force method. Mechanical of Fracture Vol. 5, Noordhoff International Publishing

Nisitani H (1983) Measure of stress field in a notch corresponding to stress intensity. Trans Jpn Soc Mech Engineers, (in Japanese), 49–447(A): 1353–1359

Noda NA, Takase Y, Kanzaki K, Nisitani H (1997) Convenient stress concentration formula useful for any shape of notch in a round test specimen (rotating bending specimen having an extremely shape V-shaped notch or an extremely blunt circular-arc notch). Trans Jpn Soc Mech Engineers, (in Japanese), 64–625(A): 2251–2257

Peterson H (1974) Stress concentration factors: charts and relations useful in making strength calculations for machine parts and structural elements. Wiley, New York

Rice JR (1968) Stresses in an infinite strip containing a semi-infinite crack. Trans ASME J Appl Mech 34: 248–249

Weibull W (1951) A statistical distribution function of wide applicability. Trans ASME J Appl Mech 18: 293–297